# Symmetric-eikonal theory of excitation with Hartree-Fock-Slater description of the target

László Gulyás
*Institute of Nuclear Research of the Hungarian Academy of Sciences (ATOMKI), P.O. Box 51, H-4001 Debrecen, Hungary*

Pablo D. Fainstein
*Centro Atómico Bariloche and Instituto Balseiro, Avenida E. Bustillo 9500, 8400 S. C. de Bariloche, Argentina*
(Received 22 November 1996)

The symmetric-eikonal model for single excitation of multielectronic targets is extended to include Hartree-Fock-Slater initial and final bound states. These wave functions are obtained by solving numerically the time-independent Schrödinger equation with a model potential. Total cross sections for excitation of He($1\,^1S$) and He($2\,^1S$) by proton impact are presented in comparison with available experimental data and other theoretical models. The model gives an accurate description at intermediate and high impact energies. Results are also presented for excitation of two-electron heavy ions and for alkaline targets.
[S1050-2947(97)00408-3]

PACS number(s): 34.50.Fa

## I. INTRODUCTION

The knowledge of accurate cross sections for different reactions in ion-atom collisions is of great importance to the study of complex systems like that of ions colliding with solid and biological targets. Also, cross sections are needed in relation to the design of heating devices for fusion plasmas. In most cases the targets are made of multielectronic atoms. If the probabilities for multiple transitions are very small, the target can be well represented with a one-active-electron model where the action of the target nucleus and the passive electrons on the active electron are represented by a model potential.

Very recently, Gulyás *et al.* [1] developed a method to include Hartree-Fock-Slater wave functions [2] in distorted-wave models for ionization. Distorted-wave models are very useful since they provide accurate results in the intermediate to high impact energy range. Together with close-coupling models, which work well at low to intermediate impact energies, they provide a description of different reactions in the full energy range.

In the present work our aim is to study the single excitation processes with a distorted-wave model in the impact energy range between 10 keV and 1 MeV. For this purpose we have chosen the symmetric-eikonal (SE) model which has been shown to reproduce experimental results for hydrogen and helium targets [3–5]. In a previous calculation with the SE model for the He target [5], analytical target wave functions were used. The initial and final bound states were represented by Roothaan-Hartree-Fock and by hydrogenic functions with variational charges, respectively. This method allows for the development of very fast codes but it presents two difficulties: (i) the bound states are not orthogonal and (ii) hydrogenic functions are not very good for excited states. With the method developed hereafter, both problems are solved and furthermore, cross sections can be calculated for any target atom in an arbitrary initial state. This can be done in a straightforward way because the initial and final bound states of the target are calculated numerically solving the time-independent Schrödinger equation with a model potential. As a by-product we obtain, from the same code, the results from the first-Born approximation.

In Sec. II we present the theoretical model. In Sec. III calculations will be presented for helium and compared with previous calculations using analytical wave function [5]. Detailed calculations are also presented in comparison with experiments and other theoretical models for excitation of helium from the ground and first excited states. Results are also presented for other targets to show the power of the method. Atomic units are used except where otherwise stated.

## II. THEORY

We consider the process where a bare ion of nuclear charge $Z_P$ and velocity $\mathbf{v}$ collides with a multielectronic target of nuclear charge $Z_T$. We assume that there is only one active electron initially in a bound state with quantum numbers $n_i l_i m_i$ which is excited to a final bound state with quantum numbers $n_f l_f m_f$ while the other electrons remain as frozen during the collision. So we solve, within the impact parameter approximation, a one-electron problem defined by the electronic Hamiltonian

$$H_{\mathrm{el}} = T_{\mathrm{el}} + V_T(x) + V_P(s), \tag{1}$$

where $T_{\mathrm{el}}$ is the electron kinetic energy operator, $V_T$ the Hartree-Fock-Slater potential of the target, $V_P$ the Coulomb interaction with the projectile, and $\mathbf{x}$ ($\mathbf{s}$) the position vector of the electron with respect to the target (projectile). In the present generalization of the symmetric-eikonal model, the initial distorted-wave function is chosen as

$$\chi_i^+ = \varphi_i(\mathbf{x})\ \ \alpha_i^+(\mathbf{s})\ \ \exp(-i\varepsilon_i t), \tag{2a}$$

$$\varphi_i(\mathbf{x}) = \frac{u_{n_i l_i}(x)}{x}\ \ Y_{l_i}^{m_i}(\hat{x}), \tag{2b}$$

 

$$\alpha_i^+(\mathbf{s})=\exp[-i\nu\ln(vs+\mathbf{v}\cdot\mathbf{s})], \tag{2c}$$

with $\nu=Z_P/v$. The function $\varphi_i(\mathbf{x})$ is an eigenstate of $H_i=T_{\rm el}+V_T(x)$ with energy $\varepsilon_i$.

The final distorted-wave function is chosen as

$$\chi_f^-=\varphi_f(\mathbf{x})\ \ \alpha_f^-(\mathbf{s})\ \ \exp(-i\varepsilon_f t), \tag{3a}$$

$$\varphi_f(\mathbf{x})=\frac{u_{n_f l_f}(x)}{x}\ \ Y_{l_f}^{m_f}(\hat{x}), \tag{3b}$$

$$\alpha_f^-(\mathbf{s})=\exp[+i\nu\ln(vs-\mathbf{v}\cdot\mathbf{s})], \tag{3c}$$

where the function $\varphi_f(\mathbf{x})$ is also an eigenstate of $H_i$ with energy $\varepsilon_f$. The functions $\alpha_i^+(\mathbf{s})$ and $\alpha_f^-(\mathbf{s})$ are the distortions in the initial and final channel and are chosen such that the initial and final states satisfy the correct boundary conditions for the Coulomb potential.

The prior version of the first-order transition amplitude as a function of impact parameter $\boldsymbol{\rho}$ is given by

$$\mathcal{A}_{if}^-(\boldsymbol{\rho})=-i\int_{-\infty}^{+\infty}dt\ \ \left\langle \chi_f^-\ \ \middle|\left(H_{\rm el}-i\ \frac{d}{dt}\right)\chi_i^+\right\rangle. \tag{4}$$

The calculation from now on follows very closely the ionization case and for comparison we use the same notation (see Ref. [1]). We repeat the main steps of the calculation for completeness. We introduce the Fourier transform of the transition amplitude

$$R_{if}(\boldsymbol{\eta})=\frac{1}{2\pi}\int d\boldsymbol{\rho}\ \ \exp(i\boldsymbol{\eta}\cdot\boldsymbol{\rho})\ \ \mathcal{A}_{if}^-(\boldsymbol{\rho}) \tag{5}$$

from which the total cross section can be obtained as

$$\sigma=\int d\boldsymbol{\eta}\ \ |R_{if}(\boldsymbol{\eta})|^2. \tag{6}$$

The Fourier transform $R_{if}(\boldsymbol{\eta})$ is

$$R_{if}(\boldsymbol{\eta})=\frac{(2\pi)^2}{v}\left[-i\ \ \frac{Z_P^2}{v}\ \ F_{1x}(\mathbf{K})F_{1s}(\mathbf{Q})\right.$$
$$\left.+Z_{\rm P}\ \ \mathbf{F}_{2x}(\mathbf{K})\cdot\mathbf{F}_{2s}(\mathbf{Q})\right], \tag{7}$$

with $\mathbf{Q}=-\mathbf{K}=\boldsymbol{\eta}+(\Delta\varepsilon/v)\hat{v}$, and $\Delta\varepsilon=\varepsilon_f-\varepsilon_i$ and $(\boldsymbol{\eta},\Delta\varepsilon/v)$ the perpendicular and parallel components of the momentum transfer $\mathbf{Q}$. The auxiliary integrals in Eq. (7) can be expressed as

$$F_{1s}(\mathbf{Q})=(2\pi)^{-3/2}\int d\mathbf{s}\ \ \exp(i\mathbf{Q}\cdot\mathbf{s})\ \ [\alpha_f^-(\mathbf{s})]^*\ \ q_v^{-i\nu-1}/s$$
$$=\frac{i\Gamma(-i\nu)\Gamma(1-i\nu)}{(2\pi)^{1/2}\beta}\left(\frac{\alpha}{\beta}\right)^{2i\nu}$$
$$\times\left[F(1)+i\nu\left(1-\frac{2\alpha v^2}{\beta^2}\right)F(2)\right], \tag{8}$$

$$\mathbf{F}_{2s}(\mathbf{Q})=(2\pi)^{-3/2}\int d\mathbf{s}\ \ \exp(i\mathbf{Q}\cdot\mathbf{s})$$
$$\times[\alpha_f^-(\mathbf{s})]^*\ \ q_v^{-i\nu-1}(\hat{s}+\hat{v})$$
$$=\frac{\Gamma(1-i\nu)^2}{(2\pi)^{1/2}\alpha\beta}\left(\frac{\alpha}{\beta}\right)^{2i\nu}$$
$$\times\left[\mathbf{Q}F(1)-i\nu\frac{2\alpha v^2}{\beta^2}\left(\mathbf{Q}-\frac{\beta}{v^2}\mathbf{v}\right)F(2)\right], \tag{9}$$

where $q_v=vs+\mathbf{v}\cdot\mathbf{s}$, $F(1)={}_2F_1(i\nu,i\nu,1;-(\eta v/\beta)^2)$, $F(2)={}_2F_1(1+i\nu,1+i\nu,2;-(\eta v/\beta)^2)$, $\alpha=Q^2/2$, and $\beta=-\mathbf{Q}\cdot\mathbf{v}$.

The $F_{1x}$ function is closely related to the form factor in the Born approximation,

$$F_{1x}(\mathbf{K})=(2\pi)^{-3/2}\int d\mathbf{x}\exp(-i\mathbf{K}\cdot\mathbf{x})[\varphi_f(\mathbf{x})]^*\varphi_i(\mathbf{x})$$
$$=\left(\frac{2}{\pi}\right)^{1/2}\ \ C_{l_f m_f}\ \ e^{iM\phi_K} \tag{10}$$

and can be easily evaluated in terms of a Fourier-Bessel transform

$$C_{l_f m_f}=\sum_l\ (-i)^l(-)^{m_i}\sqrt{\frac{(2l+1)(2l_f+1)(2l_i+1)}{4\pi}}$$
$$\times\begin{pmatrix} l & l_f & l_i\\ 0 & 0 & 0\end{pmatrix}\ \begin{pmatrix} l & l_f & l_i\\ M & -m_f & m_i\end{pmatrix}$$
$$\times\mathcal{Y}_l^M(\hat{\mathbf{K}})\int dx\ \ u_{n_i l_i}(x)\ \ j_l(Kx)\ \ u_{n_f l_f}(x), \tag{11}$$

where $\mathcal{Y}_l^m=Y_l^m\exp(-im\phi)$, $Y_l^m$ is a spherical harmonic, and $j_l$ a spherical Bessel function.

The form of the $\mathbf{F}_{2x}$ function is more involved:

$$\mathbf{F}_{2x}(\mathbf{K})=(2\pi)^{-3/2}\int d\mathbf{x}\exp(-i\mathbf{K}\cdot\mathbf{x})[\varphi_f(\mathbf{x})]^*\boldsymbol{\nabla}\varphi_i(\mathbf{x})$$
$$=\left(\frac{2}{\pi}\right)^{1/2}\ \ \mathbf{L}(\mathbf{K}). \tag{12}$$

The auxiliary function $\mathbf{L}(\mathbf{K})$ is given by

$$\mathbf{L}(\mathbf{K})=\mathbf{L}^+(\mathbf{K})e^{iM^+\phi_K}+\mathbf{L}^-(\mathbf{K})e^{iM^-\phi_K}+\mathbf{L}^0(\mathbf{K})e^{iM\phi_K}, \tag{13a}$$

$$L_x^\pm(\mathbf{K})=\pm\frac{1}{\sqrt{2}}(A_{l_f m_f}^{l_i^+ m_i^\pm}+B_{l_f m_f}^{l_i^- m_i^\pm}), \tag{13b}$$

$$L_y^\pm(\mathbf{K})=\mp iL_x^\pm(\mathbf{K}), \tag{13c}$$

$$L_z^\pm(\mathbf{K})=0, \tag{13d}$$

$$L_{x,y}^0(\mathbf{K})=0, \tag{13e}$$

$$L_z^0(\mathbf{K})=A_{l_f m_f}^{l_i^+ m_i}+B_{l_f m_f}^{l_i^- m_i}, \tag{13f}$$

with $l_i^{\pm}=l_i\pm 1$, $m_i^{\pm}=m_i\pm 1$, $M^{\pm}=M\pm 1$, $M=m_i-m_f$, and requires the calculation of Fourier-Bessel transforms including the derivative of the initial radial wave function:

$$A_{l_f m_f}^{\lambda_1\lambda_2}=\sum_l\ (-i)^l\ (l_i+1)^{1/2}\mathcal{Y}_l^m(\hat{\mathbf{K}})\begin{bmatrix} l & l_f & \lambda_1\\ m & m_f & \lambda_2\end{bmatrix}\int dx \times\frac{u'_{n_i l_i}(x)-(l_i+1)u_{n_i l_i}(x)}{x}\ j_l(Kx)\ u_{n_f l_f}(x), \quad (14)$$

$$B_{l_f m_f}^{\lambda_1\lambda_2}=-\sum_l\ (-i)^l\ l_i^{1/2}\mathcal{Y}_l^m(\hat{\mathbf{K}})\begin{bmatrix} l & l_f & \lambda_1\\ m & m_f & \lambda_2\end{bmatrix}\int dx \times\frac{xu'_{n_i l_i}(x)+l_i u_{n_i l_i}(x)}{x}\ j_l(Kx)\ u_{n_f l_f}(x), \quad (15)$$

where we have introduced the angular coefficients

$$\begin{bmatrix} l & l_f & \lambda_1\\ m & m_f & \lambda_2\end{bmatrix}=\sqrt{\frac{(2l+1)(2l_f+1)(2\lambda_1+1)}{4\pi}} \times\begin{pmatrix}\lambda_1 & 1 & l_i\\ \lambda_2 & m_i-\lambda_2 & -m_i\end{pmatrix}\begin{pmatrix} l & l_f & \lambda_1\\ 0 & 0 & 0\end{pmatrix} \times\begin{pmatrix} l & l_f & \lambda_1\\ -m & -m_f & \lambda_2\end{pmatrix}. \quad (16)$$

Finally, the expression of $R_{if}$ can be cast into the form

$$R_{if}(\boldsymbol{\eta})=\frac{4\pi Z_P^2}{v^2}\frac{\Gamma(-i\nu)\Gamma(1-i\nu)}{\alpha\beta}\left(\frac{\alpha}{\beta}\right)^{2i\nu}e^{iM\phi_K}\left\{\mathcal{A}_1\ C_{l_f m_f}+\mathcal{A}_2\ \left[-\frac{\Delta\epsilon}{v}L_z^0+\eta L_x^+ +\eta L_x^-\right]+\mathcal{A}_3\ v\ L_z^0\right\}, \quad (17)$$

where

$$\mathcal{A}_1=\alpha\left[F(1)+i\nu\left(1-\frac{2\alpha v^2}{\beta^2}\right)F(2)\right], \quad (18a)$$

$$\mathcal{A}_2=-i\left[-F(1)+i\nu\frac{2\alpha v^2}{\beta^2}F(2)\right], \quad (18b)$$

$$\mathcal{A}_3=\nu\frac{2\alpha}{\beta}F(2). \quad (18c)$$

The radial functions $u_{n_i l_i}$ and $u_{n_f l_f}$ are determined by a numerical integration of the radial Schrödinger equation with the Numerov algorithm. The Fourier-Bessel transforms (11), (14), and (15) can then be evaluated numerically using methods developed for the calculation of the usual form factor in the Born approximation [6].

## III. RESULTS AND DISCUSSION

### A. Helium target: $1\ ^1S$ excitation

Helium is the most studied multielectronic target, both for its simplicity and for its important applications. Thus there exists a large database of experimental total cross sections for proton excitation of the ground state. For these reasons, almost all theoretical models have been applied to this system, including different formulations of the SE model.

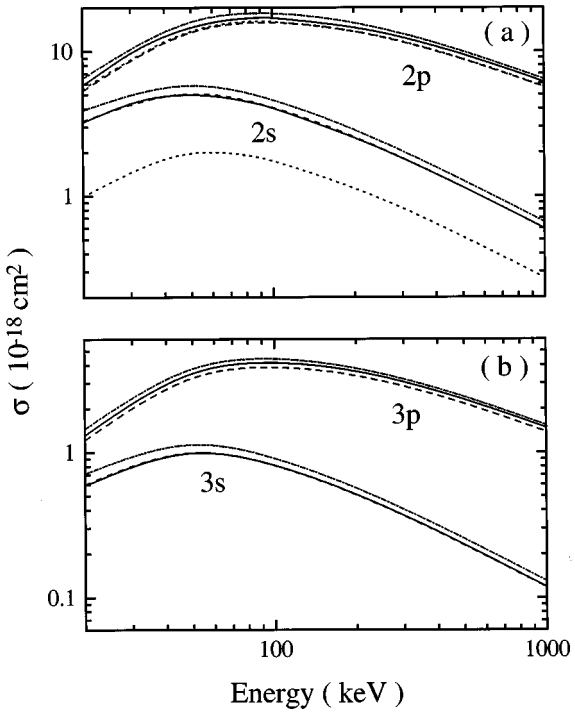


FIG. 1. Total cross section for single excitation of helium to states with principal quantum number (a) $n=2$ and (b) $n=3$ by proton impact calculated with the symmetric-eikonal model. Present results using the HS potential (dot-dashed line) [2], the GSZ potential (dashed line) [7], the HF potential (full line) [8], and results from [5] using analytical wave functions (dotted line).

Several model potentials are available for helium. These potentials give similar values of the eigenvalues. For the three potentials used here for helium we have determined that the difference between the ground state eigenvalues is less than 5%. We can then expect that such a small difference will remain between the total cross sections obtained from them. Therefore we compare in Fig. 1 calculations with the SE model using the numerical potential from Herman and Skillman (HS) [2] and the analytical potentials from Green, Sellin, and Zachor (GSZ) [7], and Opradolce *et al.* (HF) [8]. All three calculations show the same qualitative behavior and the difference between the three sets of results is less than 15%. We can then conclude that the method is stable, different potentials with small differences in binding energies produce small differences between the total cross sections. Furthermore, these differences are within the experimental uncertainties usually encountered in measurements of this process. Since in recent compilations [9–11] the experimental data for helium are normalized at high energies to theoretical calculations from the first-Born (B1) approximation, and the SE model with the same potential converges to first Born at high energies, it is of no relevance which potential we use. We can always normalize the experimental data, at high energies, to the SE or B1 calculation with a given potential. However, even if we keep this point in mind, in the present work we will always

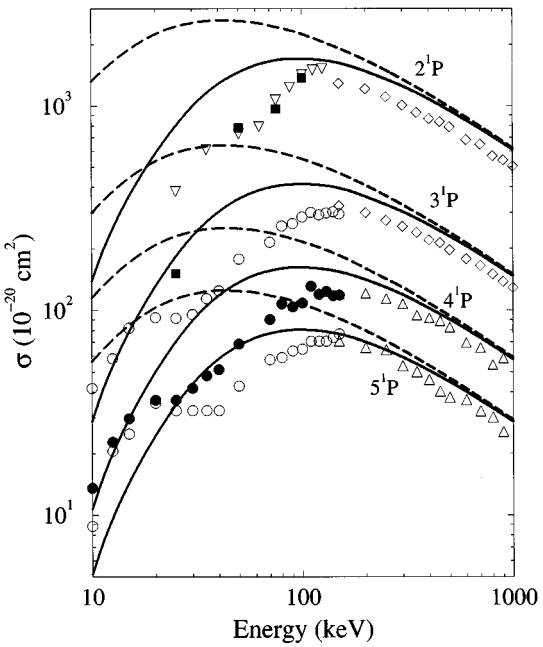


FIG. 2. Total cross section for He($1\,^1S \rightarrow n\,^1P$) excitation by proton impact. Theory: full line, present SE with HF potential; dashed line, present first-Born approximation with HF potential. Experiments: (△), from [28]; (○) and (●), from [29]; (◇), from [30]; (▽), from [31]; (■), from [32].

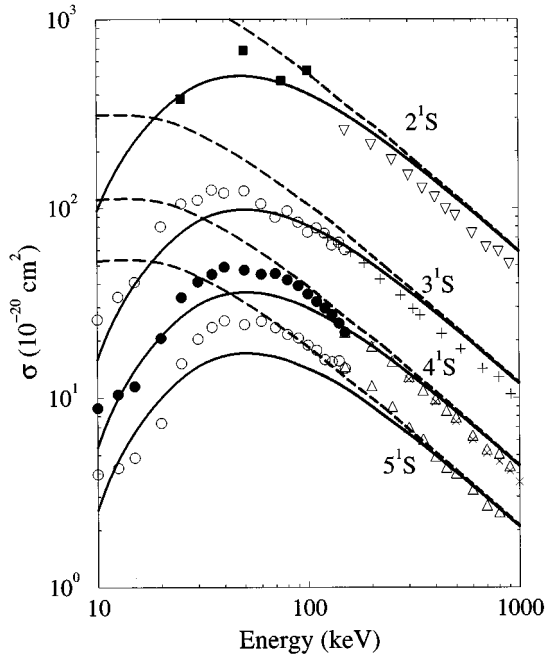


FIG. 3. Total cross section for He($1\,^1S \rightarrow n\,^1S$) excitation by proton impact. Theory: full line, present SE with HF potential; dashed line, present first-Born approximation with HF potential. Experiments: (△), from [28]; (○) and (●), from [29]; (■), from [32]; (+), from [33]; (×), from [34]; (▽), assessment of $2\,^1S$ cross sections from [9].

use the compiled values given by Fritsch [9–11] to avoid confusion.

In Fig. 1(a) we have also included results from previous calculations for helium with the SE model by Olivera *et al.* [5]. The difference between this version of the model and the one developed here is that we use more accurate wave functions for the excited states and that these wave functions are orthogonal to the ground state. Olivera *et al.* [5] use analytical wave functions for all states which, however, are not orthogonal. Excited states are represented by hydrogenic wave functions with an effective charge while here we obtain them numerically by solving the time-independent Schrödinger equation. From the figure we can see that there are large differences in the case of the $2s$ state while for the $2p$ state both calculations are very close. It appears that nonorthogonality introduces large differences for optically forbidden transitions, but these are very few calculations to conclude that this behavior will also apply for other final states.

As mentioned in Sec. I, cross sections for excitation of helium are of great importance in the design of heating devices in fusion plasmas. For this purpose, Fritsch [9–11] made a critical evaluation of the existing data for single excitation of helium to the $n\,^1P$, $n\,^1S$, and $n\,^1D$ final states ($n=2$–5) by proton impact with energies between 10 keV and 1 MeV. For almost all of these transitions and in this energy range there are experimental results available from different groups which, after suitable normalization, can be cast in a coherent set of cross sections. Much less information is available from the theoretical side where there are results only at low and high energy using the close-coupling method and the first-Born approximation, respectively [9,10]. Thus there exists a large region between the maximum of the total cross section and the region where B1 starts to be valid where there are no theoretical calculations available. Since the SE model includes higher orders from the Born series the model might prove useful to bridge the gap between the low and high energy ranges.

In Fig. 2 our present SE results for excitation to the $n\,^1P$ final states using the HF potential are compared with the available experimental data with the normalization recommended by Fritsch [9,10] and with results from the first-Born approximation which have been obtained using the same HF potential. These results are obtained from the SE code using a very small charge to cancel the distortions. It is clear from the plot that, in the region of the maximum, the SE model is in much better agreement with experiments than the B1 approximation. Still, at lower energies, the SE model overestimates the experiments and does not present the structures which are due to the coupling with the capture channel [10]. At high energies and as expected, the SE and B1 models give the same results and agree very well with the experiments. We note a systematic difference between theory and experiments at high energies which can be attributed to the fact that the experiments were normalized at high energies to the first-Born approximation with different wave functions as was discussed above. It must be noted that, very recently, a new version of the SE model was introduced by Rodríguez *et al.* [12]. In this version the one-active-electron approximation has been removed. Single configuration wave functions [13] are used for the ground and excited states which are orthogonal. Both electrons of the target are distorted in the initial and final state using eikonal phases. Results are available only for the ground state excitation to final $n\,^1P$ states by proton impact. The main differences between these cal-

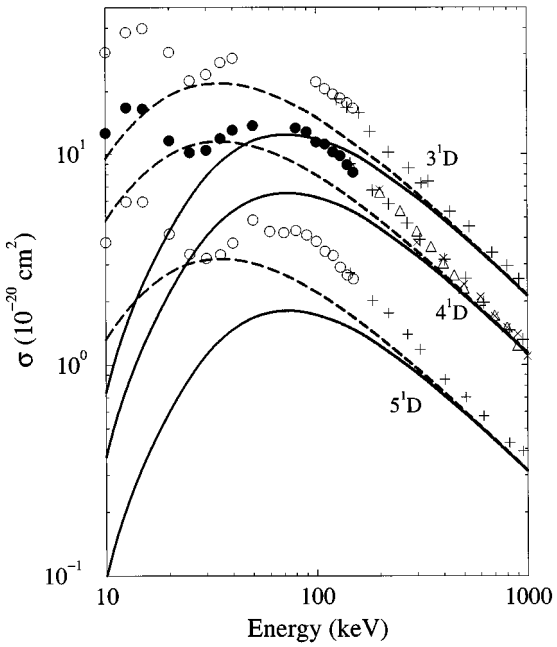


FIG. 4. Total cross section for He($1\,^1S \rightarrow n\,^1D$) excitation by proton impact. Theory: full line, present SE with HF potential; dashed line, present first-Born approximation with HF potential. Experiments: (△), from [28]; (○) and (●), from [29]; (+), from [33]; (×), from [34]. The $5\,^1D$ results were multiplied by 0.5.

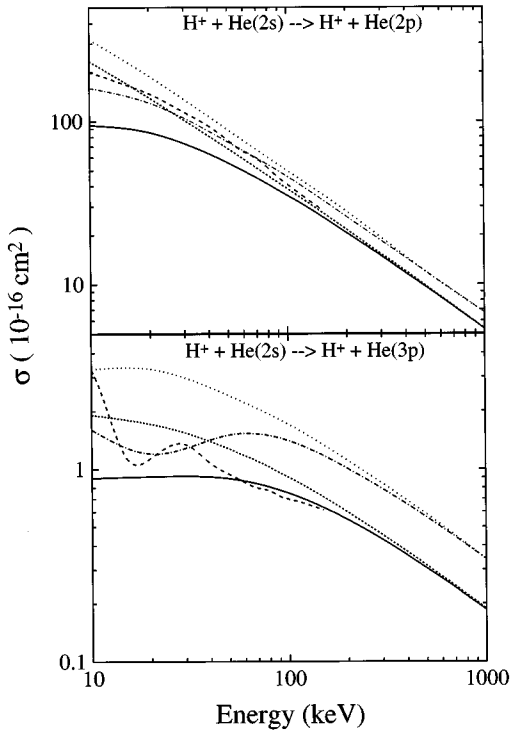


FIG. 5. Total cross section for He($2\,^1S \rightarrow 2\,^1P$) (upper curves) and He($2\,^1S \rightarrow 3\,^1P$) (lower curves) excitation by proton impact. Full line, present SE with HF potential; short-dashed line, present B1 with HF potential; dot-dashed line, Glauber approximation from [15]; dotted line, B1 from [15]; long-dashed line, close-coupling calculation from [11].

culations and the present ones appear below the maximum.

Results for excitation to the $n\,^1S$ and $n\,^1D$ final states are shown in Figs. 3 and 4. At high energies we find the same discrepancy with experiments as for the $n\,^1P$ states due to the normalization. In all cases we find much better agreement with experiments using the SE model than with the first-Born approximation. For $n\,^1P$ and $n\,^1S$ final states the agreement is quite good for energies larger than that corresponding to the maximum. On the contrary, large differences appear for the $n\,^1D$ final states. This could be due to the possibility that SE does not take account properly of second-order transitions with intermediate $n\,^1P$ states which can give significant contributions [14].

### B. Helium target: $2\,^1S$ excitation

Total cross sections for excitation of helium from the $2\,^1S$ metastable state are also needed in relation to the injection of energetic neutral beams into fusion plasmas. In this case there are no calculations available from the other versions of the SE model.

Figures 5 and 6 show the present SE and B1 calculations made using the HF potential. We have used this potential in order to compare unambiguously, at intermediate energies, with the one-electron form of the close-coupling (CC-1) calculations made by Fritsch [11]. Calculations from a two-electron (CC-2) version of that method and from the Glauber and B1 approximations [15] using single configuration wave functions [13] are also included.

The B1 and Glauber results from [15] are larger than our B1 and SE calculations due to the different wave functions. A particular case arises with the excitation to the $3\,^1P$ state where the Glauber and B1 calculations from [15] largely overestimate the CC-1 and SE calculations. This behavior has already been noted in [15], but there is no explanation available. We have calculated the excitation energies for all the transitions studied here and they are very close to those obtained from the single configuration wave functions. The differences are smaller than 15%. Thus it is not possible to attribute such a large discrepancy to the different bound states. The coupled-channel calculations (CC-2) for the $2\,^1S \rightarrow 2\,^1P$ cannot be compared directly with the present SE calculations, since they use different ways to describe the target atom. However, we can see that the two calculations join nicely above 100 keV. The same happens for the other transitions, where the coupled-channel calculations (CC-1) performed with a one-electron model description using the same model potential for helium that we use here join very well with our present results but not with the Glauber and B1 results from [15]. The SE results are smaller than the CC-1 results at lower energies. This same behavior was observed in Figs. 2–4 with respect to experiments.

### C. Heliumlike targets

Several experiments have been performed to study single and double excitation of heliumlike highly charged heavy ions at high energies. The two-electron heavy ion collides with some neutral (gaseous or solid) target which plays the role of the projectile. In some cases the target electrons can play an active role during the collision. They can be excited or even captured by the highly charged ion. However, in the present work our aim is to show the application of our method for single excitation of different atoms by bare ion

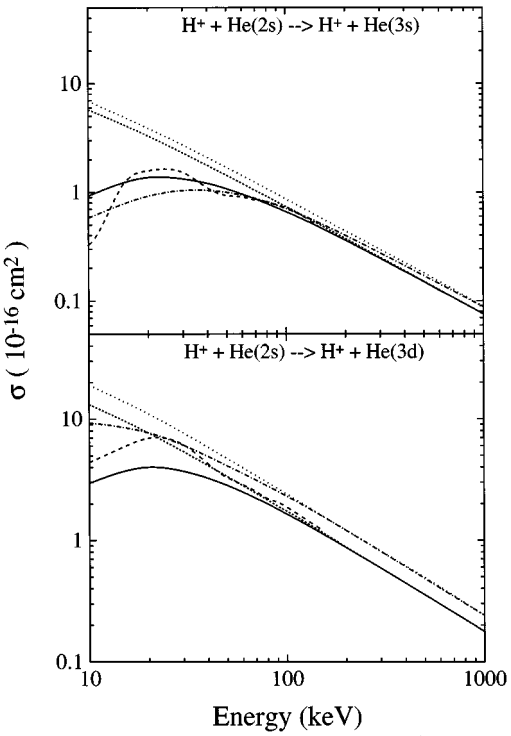


FIG. 6. Total cross section for He($2\,^1S \rightarrow 3\,^1S$) (upper curves) and He($2\,^1S \rightarrow 3\,^1D$) (lower curves) excitation by proton impact. Full line, present SE with HF potential; short-dashed line, present B1 with HF potential; dot-dashed line, Glauber approximation from [15]; dotted line, B1 from [15]; long-dashed line, close-coupling calculation from [11].

impact. Thus we will not consider here the effect of screening and thus make the approximation that the highly charged ion collides with a bare nuclei with the charge of the target nucleus ($Z_T$). The size of the screening effect has been estimated within the first-Born approximation and it contribution was found to be less than 5–8 % [5].

As a first case we consider the $1s \rightarrow 2p$ transition in the collision between $F^{7+}(1s^2)$ and $He^{2+}$ ions. Total cross sections are given as a function of impact velocity. The present SE results are obtained using a GSZ potential from [7]. In Fig. 7 these results are compared with calculations from [16] using the strong potential Born (SPB) approximation and with experimental results from [17]. The qualitative behavior of the SE and SPB models is very similar but the SE model appears to be in better agreement with experiments between 5 a.u. and 10 a.u., which corresponds to the intermediate energy regime. At low velocities the qualitative behavior of the theories is different from the experiments. The former decrease with the projectile velocity while the latter, performed with He atoms, increases as the velocity decreases. This is probably due to the contribution from the capture-ionization channel which could not be separated in the experiments from the single excitation channel and which is not taken into account in the present theoretical calculations. At high velocities, and as expected, the two theoretical models converge to the same value.

Much more detailed experiments were performed recently by Vernhet *et al.* [18] using 13.6 MeV/amu $Ar^{16+}$ ions impinging on gaseous targets with nuclear charges ranging

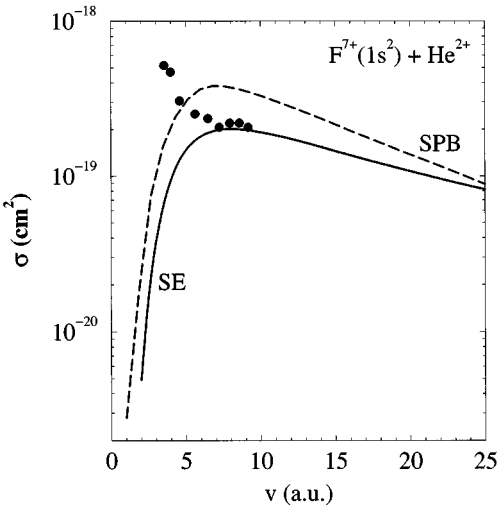


FIG. 7. Total cross section for $F^{7+}(1\,^1S \rightarrow 2\,^1P)$ excitation by $He^{2+}$ impact. Theory: full line, present SE with GSZ potential; dashed line, SPB from [16]. Experiments from [17] (●).

from 2 (He) to 56 (Xe). In these experiments it was possible, through several coincidences, to separate the contribution from different reaction channels including that of single excitation of the impinging ion. Gaseous targets were used to avoid the Stark mixing. In Fig. 8 we present our SE results for $1s \rightarrow 2p$ single excitation, obtained using the GSZ potential from [19], as a function of the target nuclear charge. In the present calculation we do not take into account the screening due to the target electrons but we make the corrections due to cascades from the $n=3$ level of the impinging ion [20]. We can see from the figure that the SE results are in good qualitative agreement with the experimental results. The theory even predicts that the cross section first increases and then decreases as a function of the target nuclear charge. This dependence has been related to the behavior of the excitation probability as a function of impact parameter [21,22]. Recent calculations for the hydrogen target with the close-coupling method using a molecular basis show the same behavior [23]. However, the absolute magnitudes are quite different. Probably, this discrepancy arises from the fact that we neglect other channels like capture ionization which can give significant contributions [18]. When the target nuclear charge increases, capture becomes very large and the interaction between the projectile electrons and the target nucleus is very strong. Thus it is possible that, except for the lightest targets, this system lies outside the range of validity of a simple perturbative approach (even if it contains higher orders of the Born series) like the present one. In fact, Lüdde *et al.* [24] have recently presented a molecular-orbital calculation of Lyman x-ray emission cross sections using single-particle amplitudes within the formalism of inclusive probabilities which takes into account the Pauli principle to calculate the multiple electron processes. These theoretical results were in very good agreement with a different set of experiments.

### D. Intrashell excitation

As a final application of the method we consider intrashell excitation of lithium ($2s \rightarrow 2p$) and sodium ($3s \rightarrow 3p$) by

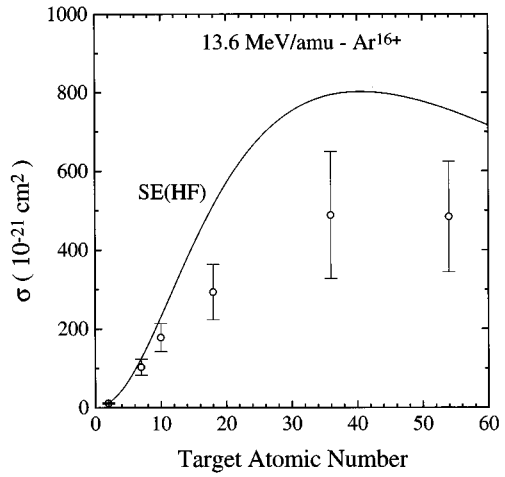


FIG. 8. Total cross section for $Ar^{16+}(1\,^1S \rightarrow 2\,^1P)$ excitation by impact on different gaseous targets with nuclear charge $Z_T$. Theory: full line, present SE with GSZ potential. Experiments from [18] (○).

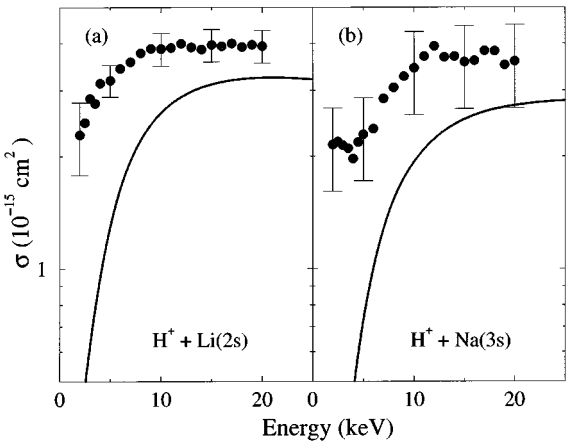


FIG. 9. Total cross section for (a) $2s \rightarrow 2p$ excitation of Li and (b) $3s \rightarrow 3p$ excitation of Na by proton impact. Theory: full line, present results with GSZ potential. Experiment: (●), for Li from [25] and for Na from [26].

proton impact. Our present results, using the GSZ potentials from [7], are shown in Fig. 9 together with experimental measurements from Aumayr and co-workers [25,26]. The experiments cover the region of intermediate to low impact energy where the single excitation and electron capture to the $n=2$ shell of hydrogen channels are strongly coupled [27]. It is then reasonable that the present results underestimate the experimental results. Atomic-orbital coupled-channel calculations (not shown in the figure) are in very good agreement with experiments [27]. The results in this figure can be compared with those for $2\,^1S \rightarrow 2\,^1P$ excitation of helium presented in Fig. 5. In that case the SE results at intermediate impact energies were smaller than the close-coupling calculations from [11]. We can then expect that the SE model will yield good results at higher energies where, at present, there are no experimental results available.

## IV. CONCLUSIONS

The symmetric-eikonal model for single excitation has been extended for arbitrary targets using numerical solutions of the time-dependent Schrödinger equation with a Hartree-Fock-Slater potential. It has been shown that different model potentials for the same target produce total cross sections which differ by the same order of magnitude as the calculated binding energies. Extensive calculations have been performed for excitation of helium initially in the ground and first-excited states. It was shown that, together with one-electron close-coupling calculations, the model provides an accurate description of the excitation cross section in the entire energy range between 10 keV and 1 MeV. Calculations were also performed for excitation of two-electron heavy ions and alkaline atoms. These applications show the power of the method which, whenever multiple transitions can be neglected, allows the study of excitation from arbitrary initial states to all final states of any target atom.

## ACKNOWLEDGMENTS

We thank Dominique Vernhet, Roberto D. Rivarola, Antoine Salin, José Luis Sanz, and Béla Sulik for helpful discussions. L.G. acknowledges financial support from the International Atomic Energy Agency (Contract No. 302-F4-HUN-8841) and the Hungarian Sciences Foundation (Grant No. T-014323). P.D.F. acknowledges financial support from Cooperativa de Electricidad Bariloche and Fundación Antorchas.

[1] L. Gulyás, P. D. Fainstein, and A. Salin, J. Phys. B **28**, 245 (1995).
[2] F. Herman and S. Skillman, *Atomic Structure Calculations* (Prentice-Hall, Englewood Cliffs, NJ,1963).
[3] G. R. Deco, P. D. Fainstein, and R. D. Rivarola, J. Phys. B **19**, 213 (1986).
[4] C. O. Reinhold and J. E. Miraglia, J. Phys. B **20**, 1069 (1987).
[5] G. H. Olivera, C. Ramírez, and R. D. Rivarola, Phys. Rev. A **47**, 1000 (1993).
[6] A. Salin, J. Phys. B **22**, 3901 (1989).
[7] A. E. S. Green, D. L. Sellin, and A. S. Zachor, Phys. Rev. **184**, 1 (1969).
[8] L. Opradolce, P. Valiron, and R. McCarroll, J. Phys. B **16**, 2017 (1983).
[9] W. Fritsch, Nucl. Fusion Suppl. **3**, 41 (1992).
[10] W. Fritsch, Phys. Lett. A **160**, 64 (1991).
[11] W. Fritsch, Phys. Lett. A **158**, 227 (1991).
[12] V. D. Rodríguez, C. Ramírez, R. D. Rivarola, and J. E. Miraglia, Phys. Rev. A **55,** 4201 (1997).
[13] T. G. Winter and C. C. Lin, Phys. Rev. A **12**, 434 (1975).
[14] F. Martín and A. Salin, in *The Physics of Electronic and Atomic Collisions*, Proceedings of the Conference held in Whistler, Canada, July, 1995, edited by L. J. Dube, B. A. Mitchell, W. McConkey, and C. E. Brion, AIP Conf. Proc. No.

360 (AIP, New York, 1995); A. Salin (private communication).
[15] A. Igarashi and T. Shirai, Phys. Scr. **T62**, 95 (1996).
[16] U. Thumm, J. S. Briggs, and O. Schöller, J. Phys. B **21**, 833 (1988).
[17] M. Terasawa, T. J. Gray, S. Hagmann, J. Hall, J. Newcomb, P. Pepmiller, and P. Richard, Phys. Rev. A **27**, 2868 (1983).
[18] D. Vernhet, J. P. Rozet, K. Wohrer, L. Adoui, C. Stéphan, A. Cassimi, and J. M. Ramillon, Nucl. Instrum. Methods Phys. Res. B **107**, 71 (1996).
[19] P. P. Szydlik and A. E. S. Green, Phys. Rev. A **9**, 1885 (1974).
[20] D. Vernhet (private communication).
[21] V. D. Rodríguez and A. Salin, J. Phys. B **25**, L467 (1992).
[22] F. Martín and A. Salin, J. Phys. B **28**, 671 (1995).
[23] A. Macías, F. Martín, A. Riera, and J. L. Sanz, Phys. Rev. A **53**, 2869 (1996).
[24] H. J. Lüdde, A. Macías, F. Martín, A. Riera, and J. L. Sanz, J. Phys. B **28**, 4101 (1995).
[25] F. Aumayr, M. Fehringer, and H. Winter, J. Phys. B **17**, 4185 (1984).
[26] F. Aumayr, M. Lakits, and H. Winter, J. Phys. B **20**, 2025 (1987).
[27] A. M. Ermolaev, J. Phys. B **17**, 1069 (1984).
[28] E. W. Thomas and G. D. Bent, Phys. Rev. **164**, 143 (1967).
[29] J. van den Bos, G. J. Winter, and F. J. de Heer, Physica **40**, 357 (1968).
[30] R. Hippler and K. H. Schartner, J. Phys. B **7**, 618 (1974).
[31] J. T. Park and F. D. Schowengerdt, Phys. Rev. **185**, A152 (1969).
[32] T. J. Kvale, D. G. Seely, D. M. Blankenship, E. Redd, T. J. Gay, M. Kimura, E. Rille, J. L. Peacher, and J. T. Park, Phys. Rev. A **32**, 1369 (1985).
[33] A. Scharmann and K. H. Schartner, Z. Phys. **228**, 254 (1969).
[34] D. Hasselkamp, R. Hippler, A. Scharmann, and K. H. Schartner, Z. Phys. **248**, 254 (1971).